

Roughness Characterization for Interconnect Analysis

Yuriy Shlepnev[#], Chudy Nwachukwu^{*}

[#] *Simberian Inc.*

^{*} *Isola*

Abstract—A novel method for practical prediction of interconnect conductor surface roughness effect on multi-gigabit digital signals is proposed. A differential impedance operator of a conductor is constructed with Trefftz finite elements and locally adjusted with a correction coefficient to account for the roughness effect. Any correction coefficient derived for the additional power loss due to roughness can be used with the proposed method. Modified Hammerstad’s correction coefficient is proposed and used here as an example. A test board is manufactured and investigated up to 50 GHz. Parameters of the conductor roughness model are identified with generalized modal S-parameters. An increase of effective dielectric constant due to conductor surface roughness is observed and explained by capacitive effect of spikes on the surface of conductor. It is shown that the constructed interconnect models are consistent with the measured data.

I. INTRODUCTION

Most of the printed circuit board (PCB) manufacturing processes use copper foils that are treated to increase surface roughness to improve adhesion to dielectrics and to avoid delamination. Appropriate electrical modelling of conductor roughness on such boards is important for accurate prediction of signal degradation effects [4]-[8], [10], [13]. Electrical characterization of roughness effect for analysis of digital and microwave signal propagation in rough PCB interconnects is the subject of this paper.

There are multiple methods available for modelling of the conductor roughness effect. One of the first numerical investigations of the roughness effect was done by Morgan in [1] for simplified surfaces with triangular and rectangular grooves. The results of [1] were fitted by authors of [2] and later published in [3]. This model is widely known as Hammerstad’s Correction Coefficient (HCC) and was successfully used for analysis of microwave circuits and recently for PCB interconnects [4], [5]. However, the reports on the model applicability for PCB interconnects are controversial [6]-[8]. The main problem of the HCC is that the maximal increase in attenuation due to conductor roughness is limited to a maximum factor of 2. Still, authors of [4]-[6] demonstrated that the model provide good accuracy for some types of copper surfaces. There have been multiple attempts to derive alternative roughness models based on the rough surface power absorption correction coefficients [6], [7],

[9] - [12]. Hemispherical approximation of rough surface was used in [6] to derive the correction coefficient. “Snowball” model was used in [7] to derive Hurray’s correction coefficient. Another correction coefficient was introduced by Sandstroem in [9] and validated experimentally in [10]. Correction coefficient called power absorption enhancement function was introduced in [11], [12] on the basis of power spectral density of the rough surface. Practically all correction coefficient models were validated with experiments, but have one common problem. It is difficult to define the model parameters for a particular case. Measurements using expensive equipment are typically required to define parameters for a particular model. Only RMS peak-to-valley value (R_q) is required for the HCC model. That value is typically available from the laminate manufacturer. The restrictive factor of 2 discussed earlier can be removed by introducing the roughness factor coefficient as is done in this paper.

Alternatively to the correction coefficient approaches, an equivalent generalized impedance boundary conditions can be applied as suggested in [15]. 3-D electromagnetic analysis of surfaces approximating rough surface can be directly used to simulate the effect of roughness as it is done in [13], [14], and [16]. A good review of the theory of rough surfaces can be found in [15] and [16]. The main problem with the equivalent boundary conditions and 2D or 3D analysis of surfaces is that we do not know what surface approximation is close to actual rough surface. That surface is technically a fractal [17] and cannot be approximated with simple shapes. Pictures in [7] illustrate that very well. Authors of [6] and [7] also pointed out that measurements with a profilometer or from micro-photographs of cross-sections may be misleading in predicting the roughness effect. Profilometer data or micro-photography may not provide sufficient resolution to observe peculiarities of the rough surface.

Finally, after studying all the cited papers, we realized that all we know about roughness is that it increases the absorption of electromagnetic energy, which is observable as an increase in attenuation and insertion losses at high frequencies. A simple heuristic model may be needed to extend the applicability of the HCC model to surfaces with different roughness profiles.

In this paper we begin with an experimental observation of the roughness effect on insertion loss and group delay in PCB interconnects made of copper foils with regular and low-profile roughness. We show that modelling such interconnects with dielectric parameters defined separately by Bereskin's method [18] produces lower insertion loss and group delay. First, we build an electromagnetic model of interconnects with the novel roughness model. A roughness correction coefficient is used for local adjustment of differential surface impedance operator constructed for conductor with Trefftz finite elements. Next, we extend the HCC model to simulate cases with possible increase in attenuation smaller and larger than 2. Parameters of such heuristic model are then extracted with the generalized modal S-parameters technique similar to identification of dielectric model parameters [19]. The suggested roughness characterization procedure is practical and can be applied for reliable prediction of interconnect behaviour for a particular laminate manufacturing process.

II. TEST BOARD RESULTS AND PRELIMINARY ANALYSIS

To investigate the effect of roughness, a PCB with 8 layer stackup has been designed and manufactured. The board in a micro-probe station is shown in Fig. 1. It has two microstrip layers (top and bottom) and 2 strip-line layers (L3, and L6). Two different copper foils and two different dielectrics are used to manufacture the board.

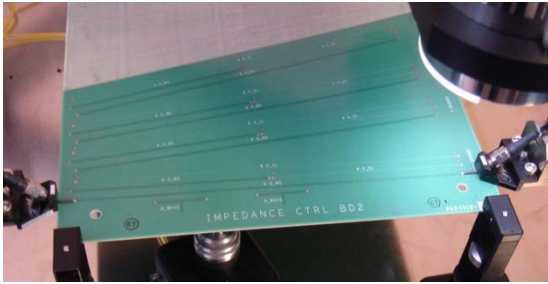


Fig. 1. Test board in the micro-probe station.

Dielectric constant (Dk) and loss tangent or dissipation factor (Df) for both dielectrics were identified in a separate experiment with accurate Bereskin's strip-line method [18] using smooth copper. The results are Dk=3.0 and Df=0.003 for I-Tera 1080 laminate (both core and prepreg) and Dk=3.3 and Df=0.0034 for 2116 laminate. The values are measured at 2, 5 and 10 GHz. Note that it is normal to have almost constant dielectric constant and loss tangent in this frequency band for these types of dielectrics with low polarization losses.

Test structures on the board are 4 and 8 inch straight microstrip and strip lines with transitions to probing pads on the surface of the board. Microstrip lines in the top layer are 8.9 mil wide strips made of very rough standard RTF/TWS copper foil on I-Tera 1080 prepreg laminate without solder mask. Strip lines in layer L3 are 4.1 mil wide strips made of TWS copper foil and sandwiched between 1080 core and prepreg laminates. Strip lines in layer L6 are 5.7 mil wide strips made of low roughness profile LP3 copper foil between I-Tera 2116 core and prepreg laminates. Microstrip lines in

the bottom layer are 12.9 mil wide strips made of LP3 copper foil on 2116 prepreg laminate. To improve accuracy of experiment, the strip widths as well as the dielectric layer thicknesses are measured after fabrication from micro-photographs of the board cross-sections.

S-parameters were measured for all transmission line segments with an Agilent VNA. The reflection loss was below -20 dB up to 20 GHz and below -10 dB up to 50 GHz. This is relatively good data, but the direct use of transmission coefficients for material property identification may introduce uncertainties due to the non-zero reflection losses. Thus, pairs of lines are used to extract reflection-less generalized modal S-parameters (GMS-parameters) of 4-inch line segments following the procedure described in [19]. GMS-parameters were additionally fitted with square root of frequency plus third order polynomial function to minimize measurement and non-identity noise (RMS fitting errors in magnitudes are less than 0.005, in phases less than 1.5 deg.). The results are plotted in Fig. 2 and Fig. 3 with stars for strip lines in layers L3 and L6 respectively.

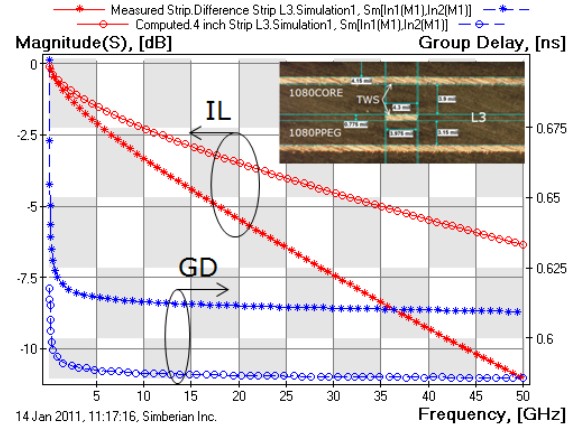


Fig. 2. Measured (stars) and preliminary computed (circles) insertion loss (IL, red curves) and group delay (GD, blue curves) of 4 inch strip line in layer L3 (foil TWS, laminate 1080).

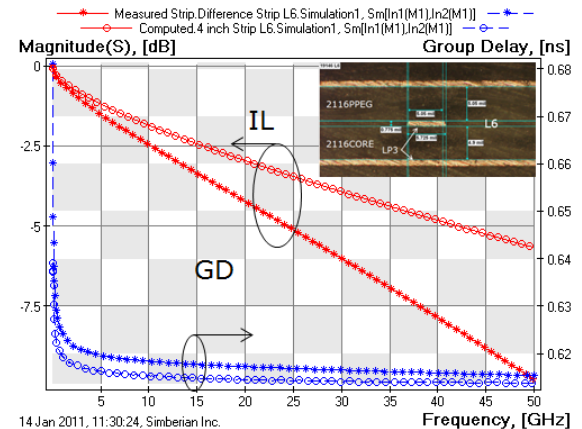


Fig. 3. Measured (stars) and preliminary computed (circles) insertion loss (IL, red curves) and group delay (GD, blue curves) of 4 inch strip line in layer L6 (foil LP3, laminate 2116).

We then computed GMS-parameters of 4-inch line segments with the dielectric parameters defined by Bereskin's

method, assuming that all conductors have smooth surfaces. We have used causal Djordjevic-Sarkar model [27] for all dielectrics with parameters defined at 2 GHz. The results are plotted with circles in Fig. 2 and Fig. 3. This preliminary computed model predicts an almost flat dielectric constant and loss tangent over the investigated frequency band. We observed substantial difference in the insertion loss for all four types of transmission lines. Group delays for microstrip line in top layer and for strip line in layer L3 (made of rough TWS foil and 1080 laminate) were also substantially different from the measured data as shown in Fig. 2 and Fig. 3. In the case of the microstrip line on the top layer, the relative difference in group delay was slightly smaller than in the case of the strip line in layer L3. Computed group delays for the microstrip line in the bottom layer and for the strip line in layer L6 (LP3 foil and 2116 laminate) were much closer to the measured data. To match the modelled and measured group delays for all four types of lines we have adjusted dielectric constants as follows: from 3 to 3.15 for 1080 prepreg and to 3.35 for 1080 core, from 3.3 to 3.36 for 2116 prepreg and to 3.25 for 2116 core. The adjustment for the 2116 laminate is within the 5% limit expected for such material. However, the adjustment for the 1080 core laminate exceeds 10%. A possible explanation is the sparse weave fibres in the 1080 laminate affecting the observed Dk which is larger due to glass-fibre effect on the stripline.

An alternate explanation is that the group delay or effective dielectric constant increases due to the roughness effect as suggested in [8] and also noted in [13]. Authors of [8] suggested that roughness increases the line inductance. However, the observed group delay is larger even at very low frequencies where there is no skin-effect and currents are uniformly distributed across the conductors. To observe such large increase in group delay and in the effective dielectric constant would require at least a 10% increase in observed total inductance per unit length. The internal inductance should be about 2 times that of theoretically predicted value for a solid copper conductor with the same cross-section at DC. The final argument against the increase in inductance is that the effect should be also visible as an increase of the characteristic impedance. Increase of the dielectric constant and hence capacitance should lead to decrease of characteristic impedance. This is exactly what we observed in this case. Characteristic impedance computed with the increased dielectric constant was in good agreement with impedance data from TDR. The difference would be about 10% if roughness increases the inductance. We have not observed such difference. Thus, **the most probable explanation of the phenomenon is simple increase of capacitance due to the spikes on the rough conductor surface.** This increase in capacitance can be especially observed for thin laminates. In our case maximal peak-to-valley value measured with profilometer was 11.3 μm for TWS and only 3.1 μm for LP3 foil. Electrical field may be nearly singular near the sharp peaks on the surface of strip similar to the strip edges. The top layer microstrip line has only one very rough surface (bottom side of the strip) and capacitance increase was only about 5%.

Strip line in layer L3 has two very rough surface (top side of the strip and plane above the strip), and corresponding capacitance increased about 10%. This is clear evidence of the capacitive effect of the roughness and it explains the large adjustment of dielectric constant for laminates facing the rough side of the conductor. Additional capacitance can be simulated either with the adjustment of dielectric constants as it is done here, or with a set of small spikes on the conductor surface as will be shown in our presentation.

Technically we can adjust the loss tangent of the dielectric and match the insertion loss in the same way as we did with the group delay. We performed this experiment and noticed that multi-pole Debye model [27] has to be used to achieve good agreement both in the insertion loss and group delay. Unfortunately, as it was pointed in [4], such model may be specific to a given trace width. Note also that the direct separation of losses might seem appealing [10], but it may not be successful for such low-loss dielectrics. As we can see from Fig. 2 and 3, the losses due to roughness are substantial and grow with frequency faster than the square root of frequency – roughness contributes to the linear term. Dielectric losses may also not be proportional to frequency due to possible increase of loss tangent with the frequency.

Thus, the natural next step is to build a computational model taking rough conductor surfaces into account and fit the model using GMS-parameters of line segment with roughness.

III. TRANSMISSION LINE MODEL WITH ROUGH CONDUCTORS

To improve the analysis of the line segment, we first build an electromagnetic model of the transmission line segment with rough conductor surface. We use a hybrid technique based on the method of lines extended to planar 3D structures in [20] and combined with the Trefftz finite elements [21] in order to simulate the interior of the conductor with rough surface. We first mesh the conductor interior with rectangular Trefftz-Nikol'skii elements with one component of electric field along the conductor and two components of magnetic field in the plane of conductor cross-section as shown in Fig. 4. Trefftz elements are built with the plane-wave solutions of Maxwell's equations in element medium as the intra-element basis functions. The intra-metal element can be described by a differential impedance matrix Z_{el} that relates local voltages (integral of electric field) and surface currents (integral of magnetic field) on the faces of element as follows [21]:

$$Z_{el} = Z_m \cdot \begin{pmatrix} \frac{\coth(\Gamma \cdot dz)}{dx} & \frac{1}{\Gamma \cdot dx \cdot dz} & \frac{\text{csech}(\Gamma \cdot dz)}{dx} & \frac{1}{\Gamma \cdot dx \cdot dz} \\ \frac{1}{\Gamma \cdot dx \cdot dz} & \frac{\coth(\Gamma \cdot dx)}{dz} & \frac{1}{\Gamma \cdot dx \cdot dz} & \frac{\text{csech}(\Gamma \cdot dx)}{dz} \\ \frac{\text{csech}(\Gamma \cdot dz)}{dx} & \frac{1}{\Gamma \cdot dx \cdot dz} & \frac{\coth(\Gamma \cdot dz)}{dx} & \frac{1}{\Gamma \cdot dx \cdot dz} \\ \frac{1}{\Gamma \cdot dx \cdot dz} & \frac{\text{csech}(\Gamma \cdot dx)}{dz} & \frac{1}{\Gamma \cdot dx \cdot dz} & \frac{\coth(\Gamma \cdot dx)}{dz} \end{pmatrix} \quad (1)$$

where $\Gamma = (1+i)\frac{1}{\delta_s}$ is the intra-metal plane wave propagation constant, $Z_m = \frac{\Gamma}{\sigma}$ is the intra-metal plane wave impedance,

$\delta_s = \sqrt{\frac{2}{2\pi \cdot f \cdot \mu \cdot \sigma}}$ is the skin depth, σ is the metal conductivity, μ is the metal permeability, f is the frequency, and dx, dz are element sizes along the X and Y axes as shown in Fig. 4.

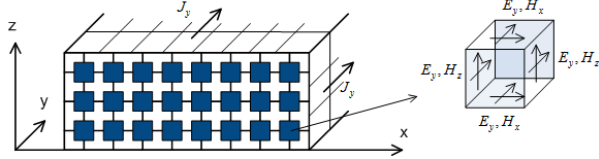


Fig. 4. Trefftz finite element model of the three-layer conductor (elements have different size along the Z-axis).

Trefftz element (1) is reciprocal and conservative at all frequencies. In addition, the element matrix (1) has correct low and high-frequency asymptotes. Skin-effect is automatically accounted for in the element formulation - element size can be much larger than the skin depth. In fact, even one element can be considered as a good approximation of a typical strip conductor. Table I shows the convergence of the real and imaginary parts of the impedance computed for a single 15 mil by 1.4 mil strip conductor with different number of elements along the wide and narrow strip sides.

TABLE I
REAL (TOP) AND IMAGINARY (BOTTOM) PARTS OF STRIP IMPEDANCE [OHM/M]

NxM	100 KHz	10 MHz	100 MHz	1 GHz
1x1	1.2726	1.3421	3.3129	10.0971
16x2	1.2726	1.3329	3.3012	10.0933
128x16	1.2726	1.3321	3.2568	10.0351
Wheeler's [25]		1.2110	3.1271	9.9028
[26]: 172x16			4.848	

NxM	100 KHz	10 MHz	100 MHz	1 GHz
1x1	0.006088	0.5859	3.1846	9.9072
16x2	0.005866	0.5771	3.1911	9.9104
128x16	0.005782	0.5685	3.1672	9.9158
Wheeler's [25]		0.5943	3.1686	9.9028
[26]: 172x16			4.0287	

Data computed with approximate Wheeler's formula and numerical results from [26] are also included into Table I for comparison. Differences with results of [26] can be explained by uncertainty in the impedance definition for a rectangular conductor. We have computed the impedance by integrating surface currents and averaging the voltage drop on the conductor surface. The introduction of a single-value voltage drop is the approximation in this case and does not impact the actual accuracy of the method. Actual voltages on the conductor surface are varying due to non-uniformity of the current in the conductor cross-section. Note that in case of a circular wire, the voltage drop is exactly identical at all locations on the surface of a conductor and thus the impedance of a circular wire can be uniquely defined, unlike the case of a rectangular conductor.

The impedance matrices Z_{el} of all the elements in conductor cross-section are simply connected, following the procedure similar to that described in [21]. A conductor

impedance matrix Z_{cs} that relates local voltages and surface currents at the surface of the conductor is formed. This procedure of connecting matrices enforces the boundary conditions between two Trefftz elements. The final matrix is a differential surface impedance operator and is similar to the admittance operator introduced in [24]. Differential surface impedance matrix is united with the grid Green's function (or matrix) [20] describing multi-layered dielectric and conductive planes and built with the method of lines. With this hybrid technique we compute admittance parameters for two segments of transmission line and extract complex propagation constant Γ_{TL} , characteristic impedance and complex impedance and admittance per unit length following the procedure introduced in [22]. With computed Γ_{TL} , generalized modal S-matrix of the line segment with length dL can be computed as:

$$Sg = \begin{bmatrix} 0 & \exp(-\Gamma_{TL} \cdot dL) \\ \exp(-\Gamma_{TL} \cdot dL) & 0 \end{bmatrix} \quad (2)$$

Matrix Sg is normalized to the complex characteristic impedance of the line and does not have reflection. In the case of coupled or multi-conductor line, such a matrix has zero modal transformation terms as shown in [19].

To account for roughness, the conductor surface impedance matrix Z_{cs} can be adjusted to simulate additional losses and inductance of the rough conductor surface. One approach is to introduce a layer of elements on the surface of the conductor with effective permittivity and permeability as suggested in [15]. Another possibility is to use a correction coefficient and adjust the cross-section impedance matrix before uniting it with the method of lines Green's operator which describes multilayered media. For that purpose, we first compute correction coefficients and place them in the diagonal elements of matrix K_{sr} and then multiply the conductor impedance matrix with the correction matrix as follows:

$$Z_{cs}^n = K_{sr}^{1/2} \cdot Z_{cs} \cdot K_{sr}^{1/2} \quad (3)$$

Matrix K_{sr} has the same dimension as the conductor cross-section impedance matrix Z_{cs} . Correction coefficients may be different for different sides of the strip. For example, if top and bottom strip sides have different roughness type or values, the corresponding correction coefficients on diagonal of K_{sr} can be adjusted to account for the differences. This will force current re-distribution in the conductor cross-section that minimizes total conductor losses. Similar surface impedance correction is used here in the spectral domain to account for roughness of plane layers. Any roughness correction coefficient introduced in [3], [6], [7], [9]-[12], [16] can be used in (3) for adjustment of the surface impedance operator. Both real and imaginary parts of the surface impedance are adjusted simultaneously. This implies that not only the resistance, but also the internal conductor inductance is

adjusted to account for the roughness. This is in accordance with the Leontovich's surface impedance boundary conditions and with the Wheeler's formula [25] that equates the real and imaginary parts of impedance for conductors with well-developed skin-effect. Table I also justifies such adjustment (see 1 GHz column). However, disproportionally large increases in the internal inductance of conductor cannot be predicted by this model. Note that the approach with correction coefficients (3) can be considered as the local version of the total resistance adjustment suggested in [5]. Typically, attenuation is adjusted with a roughness correction coefficient that leads to non-causal results.

Finally, for a practical illustration of the roughness correction algorithm we modify Hammerstad correction coefficient [3] as follows:

$$k_{sr} = 1 + \left(\frac{2}{\pi} \cdot \arctan \left[1.4 \frac{\Delta}{\delta_s} \right] \right) \cdot (RF - 1) \quad (4)$$

Where δ_s is the skin depth defined earlier, Δ is RMS peak-to-valley distance, and RF is a new parameter that is called roughness factor ($RF > 1$). RF characterizes the expected maximal increase in conductor losses due to roughness effect. Obviously, $RF=2$ gives classical Hammerstad equation [3] with maximal possible increase in conductor loss equal to 2. For further computations we will also use another form of (4) obtained by fitting numerical data for surfaces with triangular profile and implemented in Simbeor software as an alternative to the modified HCC (difference between two models is less than 10%). The algorithm described here is implemented in the electromagnetic signal integrity software Simbeor 2011 [23] used for all computations here.

IV. ROUGHNESS IDENTIFICATION WITH GMS-PARAMETERS

Here we use generalized modal S-parameters (GMS-parameters) for validation and identification of material parameters. Due to the absence of reflections, modal transformations and simplicity of the transmission term, the GMS-matrix (4) is ideally suited. No computational models of probes or launches are required. The matrix (4) can also be easily extracted from S-parameters measured for two segments of transmission line with different lengths [19].

Initially we assume that all additional losses observed originally on Fig. 2 and 3 are attributed to additional conductor losses due to roughness. To simulate the roughness effect, we will use model (4) and a similar model from the Simbeor software. There are two parameters in both models - Δ and RF . If Δ is equal to RMS peak-to-valley (R_q) as in the original HCC model, it can be measured with a profilometer. RF can also be mechanically measured as the average increase in path along the rough surface as compared to a flat surface. We used profilometer measurements and computed R_q and RF for two types of foil used on the test board: $R_q=2.6 \mu\text{m}$, $RF=1.85$ for TWS foil; $R_q=0.68 \mu\text{m}$, $RF=1.3$ for LP3 copper. Using this data, computed insertion loss was larger than measured at lower frequencies and smaller at high frequencies for microstrip in the top layer and

stripline in layer L3 made of TWS foil with both modified HCC (4) and with Simbeor model. Insertion loss was substantially lower at all frequencies for a microstrip at the bottom layer and for a strip line in layer L6 made of LP3 foil. The mechanical characterization attempt was clearly not successful and the reasons have to be further investigated. Instead, we decided to use the roughness correction coefficient and simply adjust parameters Δ and RF to achieve good correspondence with the original measured data. This procedure was more successful. With $\Delta = 0.35$ and $RF=2.8$ used for all surfaces, insertion losses for both microstrip and strip lines made of TWS copper provided a good match to the measured data as shown in Fig. 5. The computation was performed with Simbeor model. The modified HCC model also provided acceptable match with $\Delta = 0.35$ and $RF=2.6$ as shown in Fig. 6.

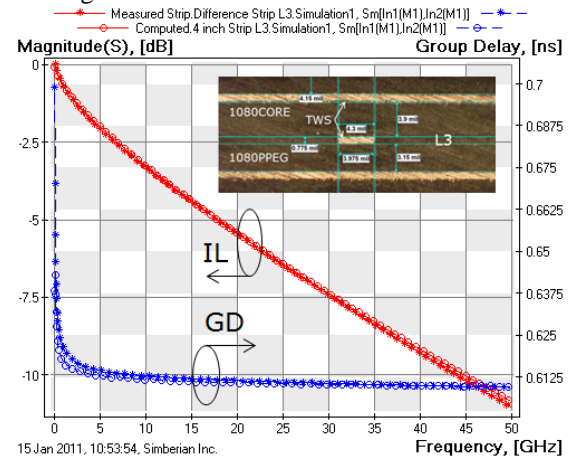


Fig. 5. Measured (stars) and modelled (circles, Simbeor roughness model) insertion loss (IL, red curves) and group delay (GD, blue curves) of 4 inch strip line in layer L3 (foil TWS, laminate 1080).

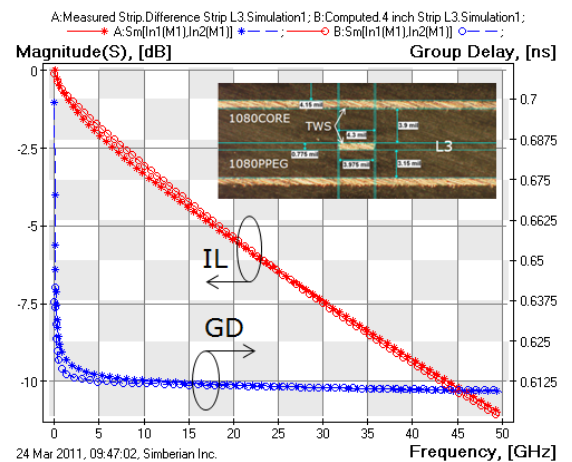


Fig. 6. Measured (stars) and modelled (circles, modified HCC roughness model) insertion loss (IL, red curves) and group delay (GD, blue curves) of 4 inch strip line in layer L3 (foil TWS, laminate 1080).

The good agreement between measured and computed group delays is due to the correction factor applied to the dielectric constants as discussed earlier in section II (from original 3 to 3.15 for prepreg to 3.35 for core 1080 laminate).

In order to match measured and simulated insertion loss for microstrip in bottom layer and strip line in layer L6 (LP3 foil) we have adjusted the roughness parameters as follows: $\Delta = 0.11$ and $RF=7$. LP3 foil showed smaller loss increase at lower frequencies (smaller Δ), but larger increase with the frequency (larger roughness factor RF). Dielectric constant adjustment for 2116 laminate with LP3 copper foil was relatively small: from 3.3 to 3.36 for prepreg and to 3.25 for core layers.

In summary, we have shown the possibility to achieve good accuracy in modelling rough interconnects with surface impedance roughness correction coefficients. One roughness model has been used for strip and microstrip lines made of the same foil and with different strip widths.

V. CONCLUSION

A new practical method for roughness characterization has been proposed in this paper. Conductor differential surface impedance operator is constructed with Trefftz finite elements and locally adjusted with a roughness correction coefficient. Hammerstad correction coefficient is modified with a roughness factor to account for variations in maximal possible increase in attenuation due to roughness. The new roughness model parameters were identified with generalized modal S-parameters. A test board was built and investigated. It was shown that the suggested approach is acceptable for analysis of interconnects on such board within some variation of trace widths at frequencies from DC to 50 GHz or with data rates up to 25-30 Gbps. Substantial increase of effective dielectric constant due to conductor surface roughness has been observed and explained by capacitive effect of nearly singular spikes on the surface of conductor.

There remains a lot of uncertainties in modeling of interconnects on PCBs. Effects like inhomogeneity of dielectrics, weave effect, relatively large variations of dimensions and roughness make accurate analysis of interconnects on PCBs extremely difficult. This paper reports work in progress; in order to further investigate roughness, we are presently building another set of test boards with different foils and more homogeneous I-Tera I-Tera using 3313, 1067 or 1086 weave.

REFERENCES

- [1] S.P. Morgan Jr., "Effect of Surface Roughness on Eddy Current Losses at Microwave Frequencies," *Journal of Applied Physics*, Vol. 20, p. 352-362, April, 1949.
- [2] E.O. Hammerstad, F. Bekkadal, *Microstrip Handbook*, Univ. Trondheim., 1975.
- [3] E.O. Hammerstad, Ø. Jensen, "Accurate Models for Microstrip Computer Aided Design", *IEEE MTT-S Int. Microwave Symp. Dig.*, p. 407-409, May 1980.
- [4] G. Brist, S. Hall, S. Clouser, T. Liang, "Non-classical conductor losses due to copper foil roughness and treatment," *2005 IPC Electronic Circuits World Convention*, February 2005.
- [5] T. Liang, S. Hall, H. Heck, & G. Brist, "A practical method for modeling PCB transmission lines with conductor roughness and wideband dielectric properties," *IEE MTT-S Symposium Digest*, p. 1780, November 2006.
- [6] S. Hall, S. G. Pytel, P. G. Huray, D. Hua, A. Moonshiram, G. A. Brist, E. Sijercic, "Multigigahertz Causal Transmission Line Modeling Methodology Using a 3-D Hemispherical Surface Roughness

- Approach", *IEEE Trans. On MTT*, vol. 55, No. 12, p. 2614-2623, Dec. 2007.
- [7] P. G. Huray, O. Oluwafemi, J. Loyer, E. Bogatin, X. Ye "Impact of Copper Surface Texture on Loss: A Model that Works", *DesignCon 2010*.
- [8] A. F. Horn III, J. W. Reynolds, P. A. LaFrance, J. C. Rautio "Effect of conductor profile on the insertion loss, phase constant, and dispersion in thin high frequency transmission lines", *DesignCon 2010*.
- [9] S. Sundstroem, "Stripline Models with Conductor Surface Roughness", *Master of Science Thesis*, Helsinki University of Technology, Finland, February 2004.
- [10] S. Hinaga, M., Koledintseva, P. K. Reddy Anmula, & J. L. Drewniak, "Effect of conductor surface roughness upon measured loss and extracted values of PCB laminate material dissipation factor," *IPC APEX Expo 2009 Conference*, Las Vegas, March 2009.
- [11] L. Tsang, X. Gu, & H. Braunisch, "Effects of random rough surfaces on absorption by conductors at microwave frequencies, *IEEE Microwave and Wireless Components Letters*, v. 16, n. 4, p. 221, April 2006.
- [12] R. Ding, L. Tsang, & H. Braunisch, "Wave propagation in a randomly rough parallel-plate waveguide," *IEEE Transactions on Microwave Theory and Techniques*, v. 57, n.5, May 2009.
- [13] Deutsch, A. Huber, G.V. Kopcsay, B. J. Rubin, R. Hemedinger, D. Carey, W. Becker, T Winkel, B. Chamberlin, "Accuracy of Dielectric Constant Measurement Using the Full-Sheet-Resonance Technique IPC-T650 2.5.5.6 " p. 311-314, .. *IEEE Symposium on Electrical Performance of Electronic Packaging*, 2002.
- [14] X. Chen, "EM modeling of microstrip conductor losses including surface roughness effect," *IEEE Microwave and Wireless Components Letters*, v. 17, n.2, p. 94, February 2007.
- [15] C. L. Holloway, E. F. Kuester, "Impedance-Type Boundary Conditions for a Periodic Interface Between a Dielectric and a Highly Conducting Medium", *IEEE Trans. on AP*, vol. 48, N 10, p. 1660-1672, Oct. 2000.
- [16] M. V. Lukic', D. S. Filipovic, "Modeling of 3-D Surface Roughness Effects With Application to -Coaxial Lines", *IEEE Trans. on MTT*, vol. 55, No. 3, p. 518-525, 2007.
- [17] D. L. Jaggard, "On fractal electrodynamics," in *Recent Advances in Electromagnetic Theory*, H.N. Kritikos and D. L. Jaggard, Eds. Berlin, Germany: Springer-Verlag, ch. 6, p. 183-224, 1990.
- [18] A.B. Bereskin, "Microwave Dielectric Property Measurements", *Microwave Journal*, v. 35, no. 7, pp 98-112., 1992.
- [19] Y. Shlepnev, A. Neves, T. Dagostino, S. McMorrow, "Practical identification of dispersive dielectric models with generalized modal S-parameters for analysis of interconnects in 6-100 Gb/s applications", in *Proc. of DesignCon 2010*.
- [20] Y.O. Shlepnev, "Extension of the Method of Lines for planar 3D structures", in *Proceedings of the 15th Annual Review of Progress in Applied Computational Electromagnetics (ACES'99)*, Monterey, CA, p.116-121, 1999.
- [21] Y.O. Shlepnev, "Trefftz Finite Elements for Electromagnetics", *IEEE Trans. Microwave Theory Tech.*, vol. MTT-50, pp. 1328-1339, May, 2002.
- [22] Y. O. Shlepnev, B. V. Sestoretzkiy, V. Y. Kustov, "A New Approach to Modeling Arbitrary Transmission Lines", *Journal of Communications Technology and Electronics*, v. 42, N 1, p. 13-16, 1997.
- [23] Simbeor 2011 Electromagnetic Signal Integrity Software, www.simberian.com
- [24] D. De Zutter, L. Knockaert, "Skin Effect Modeling Based on a Differential Surface Admittance Operator", *IEEE Trans. on MTT*, vol. 53, N 8, p. 2526-2538, 2005.
- [25] H.A. Wheeler, "Transmission Line Properties of Parallel Strips Separated by a Dielectric Sheet", *IEEE Trans. on MTT*, vol. 13, p. 72-185, March 1965
- [26] G. Antonini, A. Orlandi, C. R. Paul, "Internal Impedance of Conductors of Rectangular Cross Section", *IEEE Trans. Microwave Theory and Techniques*, vol. 47, N 7, 1999, p. 979-985.
- [27] Djordjevic, R.M. Biljic, V.D. Likar-Smiljanic, T.K.Sarkar, Wideband frequency domain characterization of FR-4 and time-domain causality, *IEEE Trans. on EMC*, vol. 43, N4, 2001, p. 662-667.